

## PVA:PEDOT:PSS:CARBON BASED NANO-COMPOSITES FOR PRESSURE SENSOR APPLICATIONS

A. S. HASAN<sup>a,\*</sup>, B. Y. KADEM<sup>b</sup>, M. A. AKRAA<sup>a</sup>, A. K. HASSAN<sup>c</sup>

<sup>a</sup>*Department of Polymer and Petrochemical Industries, College of Materials Engineering, University of Babylon, Babil, Iraq*

<sup>b</sup>*Renewable Energies department, College of Renewable Energies and Environmental Sciences, Al-Karkh University of Science, Baghdad, Iraq*

<sup>c</sup>*Material and Engineering Research Institute, Sheffield Hallam University, Sheffield, UK*

A novel pressure sensor, PVA:PEDOT:PSS: carbon-based nanocomposites has been characterized by different physical analyses and measurements. Through SEM and optical images, we notice that carbon-based materials to the PVA/PEDOT: PSS solutions change the shape of the surface and its mechanical characteristics in addition to the change of resistance and be the highest possible at carbon black ( $7.98 \times 10^{-1}$ ). XRD results show that the PVA/PEDOT:PSS: MWCNTs composite has the highest value of the strain ( $s = -0.0753$ ) and the lowest value for grain size ( $G = 1.03456$  nm). The adhesion properties, the casted drops solutions have high adhesion properties.

(Received September 28, 2019; Accepted March 12, 2020)

*Keyword:* PVA:PEDOT:PSS, Nano-composites, CNT, DFT, Pressure sensor

### 1. Introduction

These days, there is a quick evolution of high performance smart materials, just as shrewd home and web of things innovation; in this way, sensors innovation has steadily offered into individuals' lives and pulled in broad enthusiasm from researchers, particularly, inflexible pressure sensors. The flexible pressure sensors have a wide scope of uses since they have amazing mechanical and electrical properties, for example, high adaptability, high affectability, high goals proportion, furthermore, fast reaction, among others [1]. Concentrates on flexible, wearable sensor apparatuses have been quickly expanding in the most recent decade.

In the most recent decade, flexible devices exhibited incredible potential in different fields[2]. One of the most significant applications is a flexible electronic skin (E-skin) for pressure detecting, which is initially presented with polymer-based exchanging lattices for showcases, robots, and others [2,3]. As of late, many survey papers concentrated for the most part on the improvement of flexible electronic devices for E-skin [3–5].

The kind of pressure sensor assumes an imperative job in work productivity and execution. Particularly, the absence of the high performance in pressure or power sensor is a noteworthy obstruction [6]. Most pressure sensors are just skilled in working at high-pressure ranges. Along these lines, more research is being completed in the evolution of sensors for low-pressure ranges [7,8]. Delicate polymers like polydimethylsiloxane (PDMS) are picking up enthusiasm for micro-fluidics and sensors on account of their high adaptability, capacity to be organized into wanted shape and size, and above all, their ability to deliver savvy materials by fusing nanofillers.[8,9] The way toward blending such nanocomposite-based smart materials are significantly testing as a result of two parameters: homogeneity and stability. Fitting the essential handling steps is still a key research center, which is definitive for showing signs of improvement, more brilliant and touchy materials for pressure sensors with superior. From the sensor point of view, the decision of nanofillers in the polymer network is urgent, as it contributes to the conductivity improvement of the protecting polymer just as different electrical parameter changes in the material, affected by the outside physical or compound changes [7,10]. The conductive

---

\* Corresponding author: dmamah73@gmail.com

polymeric nanoparticle of a watery- base, Poly(3,4-ethylenedioxythiophene)-poly(styrenesulfonate) (PEDOT:PSS), has properties of adaptability, cost-effectiveness, lightness, and great electrical properties. These features give this material big importance for application in adaptable gadgets, sensors, and energy gathering/stockpiling frameworks [9,11]. The characteristic features of the stated nanoparticles above such as great conductivity, and magnificent hybridization capacity with different materials are due to its aqueous-base [7,11].

In this paper, we introduce a new type of stretchable pressure sensor from PVA:PEDOT:PSS:carbon based nano-composites. With controlling the concentration of the additive DI water, the conductivity of PVA:PEDOT:PSS:carbon based nano-composites were within range of  $1.54 \times 10^{-4}$  to  $1.00 \times 10^{-2}(\Omega \text{ cm})^{-1}$ , which is quite adequate for different applications. Due to these characteristics, the present work means to investigation of the impact of PEDOT:PSS fixation structure, electrical conduction, resistivity, adhesion and mechanical properties of PVA.

## **2. Materials and experimental methods**

### **2.1. Theoretical methods**

The PVA/PEDOT:PSS molecule was designed for the Gaussian View software using the PM6 - semi-empirical method as shown in Fig.1-A and then the study of the black carbon on the main molecule using Gaussian 09 package [12] As in Fig.2B.

The addition of SWCNTs and MWCNTs was also designed on the main molecule As in Fig.1C-D, and study the mechanical and electronic properties of all these molecules.

Through theoretical calculations, we observe a good correlation with the experimental results of electrical conductivity as in Table (1), this difference in conductivity for the samples is due to the reduction of its work function, Also note that stress is the greatest value when using MWCNTs, This indicates the high correlation of chemical bonds between PVA/PEDOT:PSS and MWCNTs as shown in Table 2.

### **2.2. Preparation methods**

Solution casting method is well-known as a simple technique usually used to produce self-standing polymer electrolyte films. 5gm of PVA (polymer) was dissolved in 50ml DI water, the water was first heated under stirrer and the PVA was added slowly to the DI water under stirrer and left for 2h at  $70^{\circ}\text{C}$  until the solution became transparent and homogeneous. Afterward, PEDOT:PSS solution was added to the PVA solution with a specific concentration followed by sonication for about 1h inside the ultrasonic bath. Later, carbon based materials (carbon black (CB), single wall carbon nanotube (SWCNTs) and multi wall carbon nanotube (MWCNTs)) were added to the PVA/PEDOT:PSS solutions to study the effect of these carbon based materials on the properties of PVA/PEDOT:PSS composites. The samples were prepared by casting method into a Petri dish and left for 2 days to obtain efficient drying at room temperature yielding a free standing, thick polymer electrolyte film. Fig.2. shows the PVA:PEDOT:PSS-based composite before and after adding carbon based materials. Another set of samples was deposited onto Si substrates for the Hall measurements using a drop casting technique, whereas another set of samples were drop casting onto IDE for the electrical conductivity. The main samples in the Petri dish were then twisted to obtain a wire shape of these composites for further characterization.

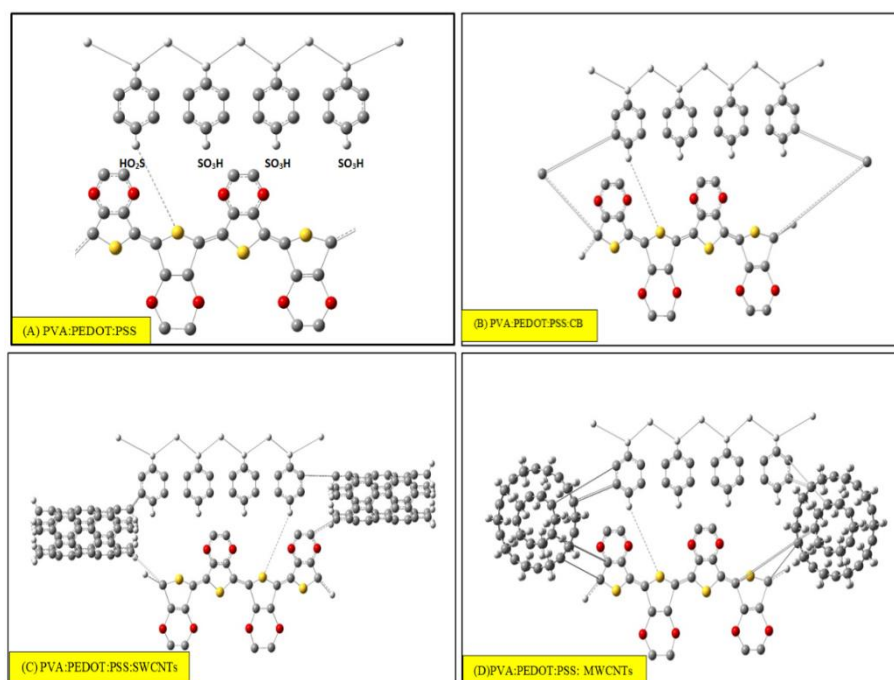


Fig. 1. Molecular geometry of (A) PVA:PEDOT:PSS, (B) PVA:PEDOT:PSS:CB, (C) PVA:PEDOT:PSS:SWCNTs, (D) PVA:PEDOT:PSS:MWCNTs.

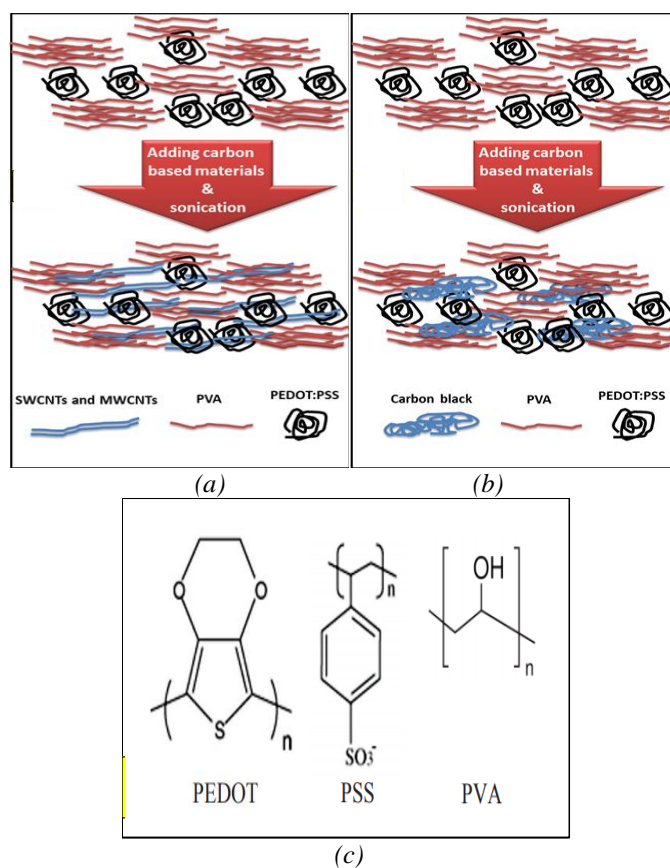


Fig. 2. PVA:PEDOT:PSS with and without adding carbon based materials (a) SWCNTs and MWCNTs and (b) CB (c) the molecular structure of PEDOT, PSS and PVA.

### 2.3. Characterization

The composite samples were characterized using different techniques. Keithley source meter 2401 was used to measure the electrical conductivity of the pre-prepared samples on Interdigitated platinum electrodes (IDEs) purchased from DropSens (Spain) (see Fig.3 (A) and (B)). The IDE can be used to measure the surface conductivity ( $\sigma$ ) of the samples from the following relationship [13]:

$$\sigma = \frac{I}{V} \left( \frac{n}{WtL} \right) \quad (1)$$

where,  $t$  is the thickness of the film ( $\sim 100$  nm),  $W$  is the overlapping distance between the fingers (6.67mm),  $n$  is the number of fingers (500), and ( $L$ ) is the distance between electrodes ( $5\mu\text{m}$ ). Hall measurements were carried out using integrated experience unit for the pre-prepared samples on Si substrates unit for the pre-prepared samples on Si substrates. Contact angle measurements were performed using Data-physics OCA15EC Goniometer with a very slow rate at room temperature. The time dependency was recorded through programmable software and the change in the voltage and resistance with time was carefully recorded.

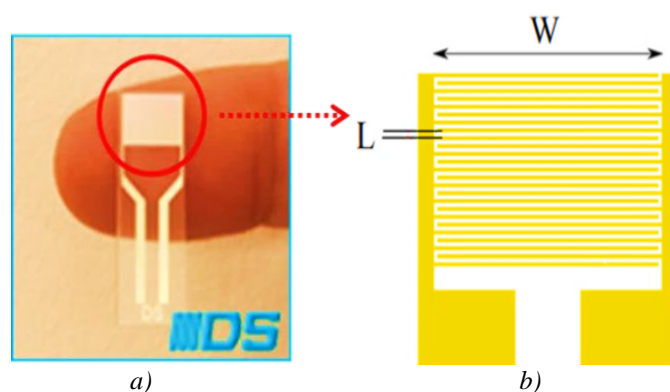


Fig. 3. (a) Interdigitated electrode (IDE) and (b) the outline scheme of the IDE.

## 3. Results and discussions

### 3.2. SEM and optical images

The scanner electron microscopy is one of the types of electronic microscopes, which gives a three-dimensional image of the sample in the most accurate detail, the effect on SEM as a major role in understanding the nature of prepared PVA/PEDOT:PSS solutions, the information obtained from the SEM image is the form and size of activated charcoal crystals, as well as the outer shape of the recorded charcoal. Fig. 4 show the SEM image. By adding the percentage of carbon based materials to the PVA/PEDOT:PSS solutions we notice that a change was made in the microstructure Moreover, a change in the grain size and the expanded gel until it fills all the spaces. The Fig.(3) shows Scanning electron microscope images of PVA/PEDOT:PSS solutions and carbon based materials. The samples were viewed at different magnification like 2,00 kX and the particles were approximately in the range of 1 to 2 nm. The SEM image clearly indicates the particles were agglomerated and they formed regular Shape. Also note, some particles were shaped like a rod and some clusters are present, individual clusters do not extend for more than a few microns [10,14].

And this illustration is similar to the images of the optical microscope Fig. 5, where we note the presence of surface-based formulations of the samples because of the difference of chemical reactions between additives and the PSS-rich areas exhibit a granular structure, and this confirms FTIR calculations of samples of the presence of creep and the difference of bonds[9].

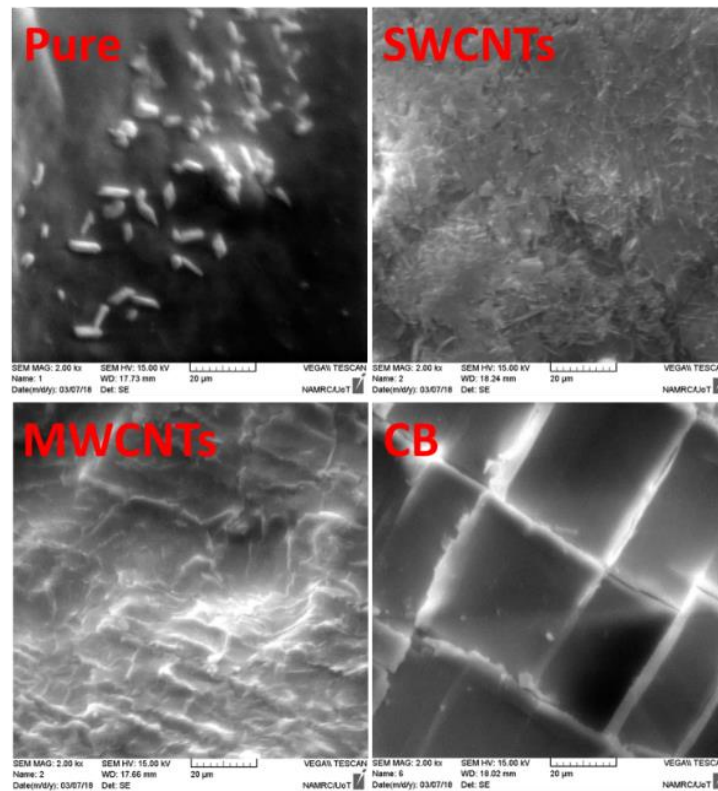


Fig. 4. SEM Images of PVA/PEDOT:PSS/carbon based materials, pure (without carbon), SWCNTs, MWCNTs and Carbon black from left to right.

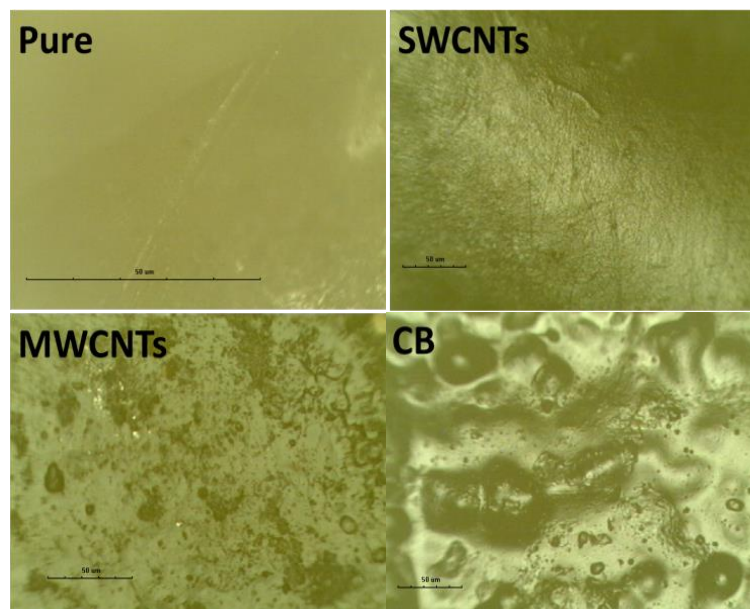


Fig. 5. optical Images of PVA/PEDOT:PSS/carbon based materials, pure (without carbon), SWCNTs, MWCNTs and Carbon black from left to right.

### 3.2. Electrical conductivity and resistivity

The electrical characteristics have been carried out in two different methods, two electrode conductivity using IDE and four point conductivity using Hall Effect experiment. The electrical conductivity has increase upon loading the carbon based materials within the PVA:PEDOT:PSS

composite wires, see Table (1) and Fig. 6. The electrical conductivity has increased from  $1.63 \times 10^{-4} (\Omega \text{ cm})^{-1}$  (Hall) and  $1.54 \times 10^{-4} (\Omega \text{ cm})^{-1}$  (IDE) to  $1.25 \times 10^{-2} (\Omega \text{ cm})^{-1}$  (Hall) and  $1 \times 10^{-2} (\Omega \text{ cm})^{-1}$  (IDE). This increase in the electrical conductivity has correlated to the introduction of percolation pathways for the charges created by carbon nanomaterials. Furthermore, the sheet resistivity has demonstrated similar trend to the electrical conductivity, however, MWCNTs has shown the lowest sheet resistance with  $0.1 \text{ M}\Omega/\text{sq}$  m compares to  $3.1 \text{ M}\Omega/\text{sq}$  for the PVA:PEDOT:PSS based wire [15,16].

Table 1. The electrical properties of the studied PVA:PEDOT:PSS-based wires.

	Hall effect		Conductivity $(\Omega \text{ cm})^{-1}$	
	Resistivity $(\Omega \text{ cm})$	sheet resistivity $\text{M}\Omega/\text{sq}$	Hall effect	IDE
Pure	$6.12 \times 10^{-3}$	3.1	$1.63 \times 10^{-4}$	$1.54 \times 10^{-4}$
SWCNTs	$3.94 \times 10^{-2}$	0.2	$2.54 \times 10^{-3}$	$2.54 \times 10^{-3}$
MWCNTs	$2.10 \times 10^{-2}$	0.1	$4.77 \times 10^{-3}$	$4.21 \times 10^{-3}$
CB	$7.98 \times 10^{-1}$	0.4	$1.25 \times 10^{-2}$	$1.00 \times 10^{-2}$

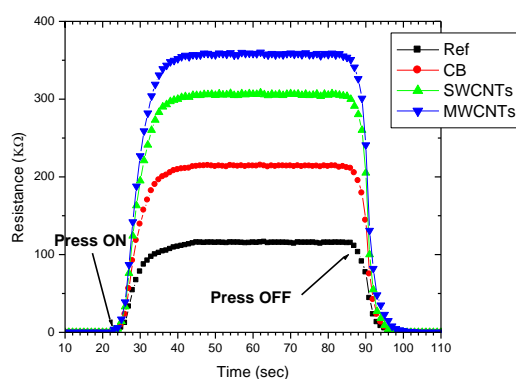


Fig. 6. The resistivity of the studied PVA:PEDOT:PSS-based wires.

### 3.3. Adhesion and mechanical properties

The adhesion properties were carried out using contact angle measurements for the solutions. All the casted drops solutions have shown relatively low contact angles which demonstrate the good adhesion properties, however, CB based material has shown better adhesion properties than other samples which can help in the application using spin coating method[17].

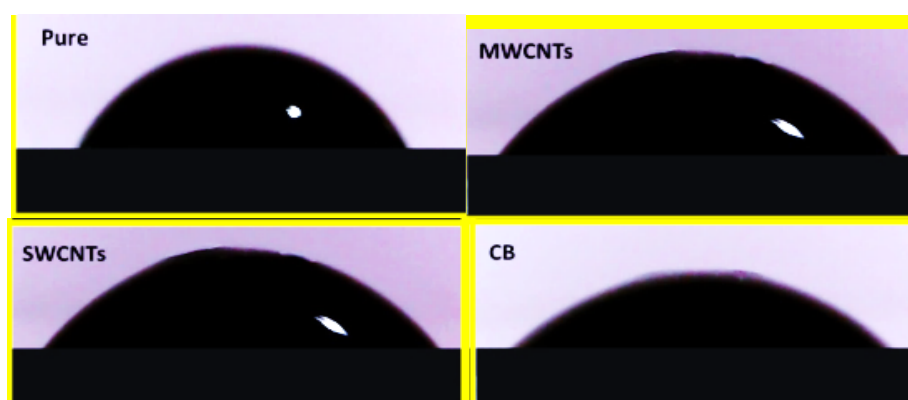


Fig. 7. Contact angle measurement on glass substrates.

### 3.4. FTIR results

Fig. 8 show the Fourier transformed infrared spectroscopy (FTIR) analysis (infrared spectra were measured at the wavelength in the range of  $400\text{-}4000\text{ cm}^{-1}$ ) of PVA/PEDOT:PSS solutions and carbon based materials :

It is observed that the bonds appear in both samples and in the different frequency values. This means that there is a chemical reaction between the solutions and carbon based materials, but there is a physical reaction from the observation of the increase in the intensity values of transmissions. The FT-IR spectra showed the characteristic asymmetrical stretching transmission peak for MWCNTs -PVA/PEDOT:PSS composites. While the lowest permeability value for CB-PVA/PEDOT:PSS composites. The (FTIR ) spectra were recorded. Also, the Fig.8, showed that the presence of the expected function groups, for example the emergence of several peaks between (1579 - 1495) related to bending group of (C=C) aromatic. We can see that the small change in intensity of the C=C band gradually became stronger [14].

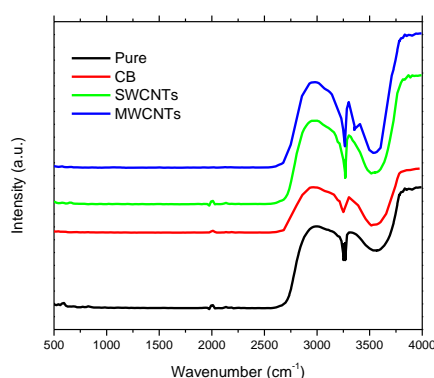


Fig. 8. FT-IR spectra of the PVA/PEDOT:PSS solutions and carbon based materials composite.

### 3.5. XRD

Fig. 9 shows the X-ray diffraction spectra for blends at different carbon based materials. The crystalline structure of the PVA/PEDOT:PSS solutions and carbon based materials can be identified by studying the phase of that substance. When a beam of X-ray incident on the surface of the thin film, the peaks appear on specific angles due to the reflection of Bragg on the surface of the parallel crystal. It is clear from Fig.9 that the crystalline structure of the prepared thin film was crystalline and remain crystallized after addition carbon based materials. The strongest peak at  $2\theta = 24.70^\circ$  in Fig. (8) corresponds to the (0 0 2) plane of the semi-crystalline carbon. At solutions all blends exhibit an additional smaller peak at  $2\theta = 25.80^\circ$  in Fig. 9 which corresponds to the (020) plane of PEDOT:PSS. This confirms the chemical compatibility of the composite, as the grain size did not change significantly when the components change and thus confirms the applicability of the compound applications pressure sensors to approximate the structural distance and high atomic order of atomic levels. Through the results of strain we note that PVA/PEDOT:PSS: MWCNTs composite has the highest value of the strain ( $s = -0.0753$ ) and the lowest value for grain size ( $G = 1.03456\text{ nm}$ ), this is the best composite for use in the applications of the pressure sensor[10,18].

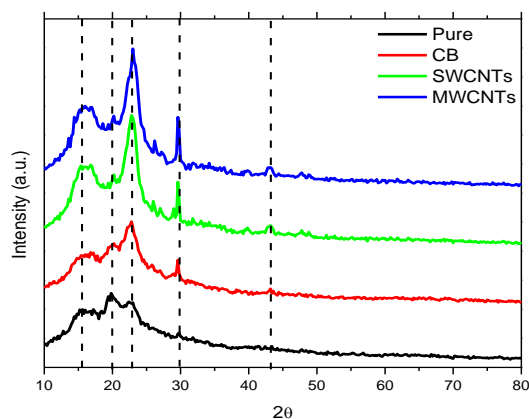


Fig. 9. X-ray diffraction pattern of the PVA/PEDOT:PSS solutions and carbon based materials composite.

Table 2. The strain and the grain size of the PVA/PEDOT:PSS solutions and carbon based materials composite.

P	CB	SWCNT	MWCNT
s= - 0.0639	s= - 0.053	s= - 0.0236	s= - 0.0753
G=1.27241	G=1.08243	G=2.21078	G=1.03456

#### 4. Conclusions

A novel fully packaged pressure sensor from PVA:PEDOT:PSS:carbon based nanocomposites has been demonstrated. Results (x-ray diffraction, SEM and optical images) show the change of morphological properties by change carbon based materials. The FT-IR spectra showed the characteristic asymmetrical stretching transmission peak for MWCNTs-PVA/PEDOT:PSS composites. The highest resistance was at carbon black ( $7.98 \times 10^{-1}$ ). The increase in electrical conductivity is due to the introduction of filtration pathways for charges resulting from carbon nanomaterials. The adhesion properties, all the casted drops solutions have shown relatively low contact angles which demonstrate high adhesion properties.

#### Acknowledgments

We would like to thank the Material and Engineering Research Institute, Sheffield Hallam University to support this study and Nanotechnology & Advanced Material Research Center, University of Technology.

#### References

- [1] C. Cochrane, M. Lewandowski, A. V. Koncar, *Sensors* **10**(9), 8291 (2010).
- [2] C. Pang, C. Lee, K. Y. Suh, *Journal of Applied Polymer Science* **130**(3), 1429 (2013).
- [3] M. L. Hammock, A. Chortos, B. C. K. Tee, J. B. H. Tok, Z. Bao, *Adv. Mater.* **25**(42), 5997 (2013).
- [4] G. Massaglia, A. Chiodoni, S. L. Marasso, C. F. Pirri, M. Quaglio, *J. Nanomater.*, (2018).
- [5] X. Wang et al., *Adv. Mater.* **27**(14), 2324 (2015).
- [6] A. Chortos, Z. Bao, *Materials Today* **17**(7), 321 (2014).



- [7] A. Nag, B. Menzies, S. C. Mukhopadhyay, *Sensors Actuators, A Phys.* **276**, 226 (2018).
- [8] J. Zhang, L. Zhou, H. Zhang, Z. Zhao, S. Dong, S. Wei, J. Zhao, Z. Wang, B. Guo, P. Hu, *Nanoscale* **10**(16), 7387 (2018).
- [9] X. Fan, N. Wang, J. Wang, B. Xu, F. Yan, *Mater. Chem. Front.* **2**(2), 355 (2018).
- [10] S. M. Kim, C. Kim, Y. Kim, N. Kim, W. Lee, E. Lee, D. Kim, S. Park, K. Lee, J. Rivnay, M. Yoon, *Nat. Commun.* **9**(1), 3858 (2018).
- [11] Y. Ko, J. Kim, H. Y. Jeong, G. Kwon, D. Kim, M. Ku, J. Yang, Y. Yamauchi, H. Y. Kim, C. Lee, J. You, *Carbohydrate polymers* **203**, 26 (2019).
- [12] M. J. Frisch, *Gaussian09 Revision D.01*, Gaussian Inc. Wallingford CT, Gaussian 09 Revision C.01. (2010).
- [13] L. H. D. Skjolding, C. Spegel, A. Ribayrol, J. Emnéus, L. Montelius, *Journal of Physics: Conference Series* **100**(5), 052045 (2008).
- [14] K. H. Choi, M. Sajid, S. Aziz, B. S. Yang, *Sensors Actuators A Phys.* **228**, 40 (2015).
- [15] N. Trifigny, F. M. Kelly, C. Cochrane, F. Boussu, V. Koncar, D. Soulat, *Sensors* **13**(8), 10749 (2013).
- [16] J. Zhou, G. Lubineau, *ACS applied materials & interfaces* **5**(13), 6189 (2013).
- [17] J. L. Hmar, *RSC Adv.* **8**(36), 20423 (2018).
- [18] C. Chen, A. Torrents, L. Kulinsky, R. Nelson, M. Madou, L. Valdevit, J. LaRue, *Synthetic Metals* **161**(21-22), 2259 (2011).